Optimal Sensor Scheduling for Resource-Constrained Localization of Mobile Robot Formations

Anastasios I. Mourikis and Stergios I. Roumeliotis

***Abstract*— This paper addresses the problem of resource allocation in formations of mobile robots localizing as a group. Each robot receives measurements from various sensors that provide relative (robot-to-robot) and absolute positioning information. Constraints on the sensors' bandwidth, as well as communication and processing requirements, limit the number of measurements that are available or can be processed at each time step. The localization uncertainty of the group, determined by the covariance matrix of the equivalent continuous-time system at steady state, is expressed as a function of the sensor measurements' frequencies. The trace of the weighted covariance matrix is selected as the optimization criterion, under linear constraints on the measuring frequency of each sensor and the cumulative rate of the Extended Kalman filter updates. This formulation leads to a convex optimization problem (semidefinite program) whose solution provides the sensing frequencies, for each sensor on every robot, required in order to maximize the positioning accuracy of the group. Simulation and experimental results are presented that demonstrate the applicability of this method and provide insight into the properties of the resource-constrained cooperative localization problem.**

***Index Terms*— Robot Formations, Multirobot Localization, Resource-constrained Localization, Sensor Scheduling, Semidefinite Program,**

I. Introduction

A large number of applications require robots to move in a coordinated fashion, in order to accomplish a certain task (e.g., object moving [1], surveillance [2], platooning for efficient transportation systems [3], formation flying [4], and spacecraft formations [5]). In particular, the case in which the members of a robotic team maintain constant relative positions as they traverse the space, offers certain advantages, such as simplified motion control, collision avoidance, and the ability to collectively manipulate objects in the environment. Due to the increased versatility that robot formations provide, they have recently attracted significant interest in the mobile robotics community.

In this paper, we address the problem of *Cooperative Localization* (CL) in robot formations. Several estimation techniques have been applied to the CL problem, such as Extended Kalman Filtering (EKF) [6], Least Squares Estimation [7], Particle Filtering [8], etc. In this paper, we study the problem of determining sensing strategies that maximize localization accuracy, and for this reason employ an EKF approach, similar to the one presented in [6]. The EKF was chosen for our work because it encompasses a well-studied mechanism, the Riccati equation, for propagating the covariance matrix of the pose estimates through time. Thus, it provides us with a theoretically sound metric of localization accuracy.

Roumeliotis and Bekey [6], have shown that proprioceptive measurements from the robots' odometry sensors can be processed locally by each robot to propagate its own pose estimates. However, every time an exteroceptive measurement is received by any of the robots in the formation, *all* robots must communicate their current pose estimates. Additionally, the measuring robot must transmit its new measurement in order for the EKF update to be performed. Therefore, every exteroceptive measurement that is processed incurs a penalty in terms of use of both communication bandwidth and CPU time, as well as in terms of power consumption. In a realistic scenario, the robots of a team will need to allocate computational and communication resources to mission-specific tasks and this may force them to reduce the number of measurements they process for localization purposes. Moreover, the finite battery life of robots imposes constraints on the amount of power that can be used for tracking their position. The limitations on the available resources may thus prohibit the robots from registering, transmitting, and processing all measurements available at every time instant.

It is clear that whether or not an exteroceptive measurement should be processed in an EKF update, is determined by a tradeoff between the value of the localization information it carries, and the cost of processing it. In this paper, we assume that the robots process each of the available measurements at a constant frequency, and we seek the *optimal measurement frequencies*, in order to attain the highest possible positioning accuracy. The key element in our analysis is the derivation of an *equivalent continuous-time system model* for the robot team, whose noise parameters are functionally related to the frequency of the measurements. This enables us to express the covariance matrix of the pose errors as a *functional relation* of the frequencies, and thus to formulate the problem of determining the optimal sensing strategy as an optimization one. An important result that we prove is that this is a *convex optimization problem* and therefore it is possible to compute a globally optimal solution, using very efficient algorithms.

In addition to satisfying application-imposed constraints on communication, power, and processing resources, the results of this work may also be employed to reduce the cost of a robot team design. Specifically, if measurements from certain active sensors (e.g., lasers) are processed at a low rate, it may be possible to replace these particular sensors with slower (and cheaper) ones. Finally, in the event that the utilization frequency of a specific sensor is determined, through the optimization process, to be approximately zero, this sensor

This work was supported by the University of Minnesota (DTC), the Jet Propulsion Laboratory (Grant No. 1251073, 1260245, 1263201), and the National Science Foundation (ITR-0324864, MRI-0420836).

The authors are with the Dept. of Computer Science and Engineering of the University of Minnesota. E-mails: {mourikis|stergios}@cs.umn.edu.

can then be excluded from the payload of the host robot, thus reducing the total cost for equipping the robot group.

The rest of the paper is structured as follows: In the following section, we outline relevant approaches that appear in the literature. In Section III, the formulation of the localization problem is presented. In Section IV, we show how the measurement frequencies are related to the localization accuracy of the robots. Section V describes the formulation of the optimization problem, and in the following sections, we present experimental and simulation results that demonstrate the application of this method to several example cases. Finally, in Section VIII the conclusions of this work are drawn and future research directions are suggested.

II. Related Work

In [9], [10], [7], localization algorithms for recovering the *relative* poses between the robots in a formation, using omnidirectional cameras as the primary sensors, are described. The authors propose suboptimal estimation algorithms for achieving efficient implementations. These are derived by either considering that each robot localizes using only relative position measurements to a "leader" robot in the team, or by decoupling the problems of orientation and position estimation. In presenting these methods, the trade-offs that exist between localization accuracy and the overhead for communicating and processing relative position measurements are pointed out by the authors. However, no analysis is conducted to reveal the effect of the varying available resources on positioning uncertainty, and no optimal sensing strategies are proposed.

The impact of the *geometry* of a robot formation on localization accuracy has been addressed in previous work. Specifically, the case of a *static* formation is studied in the work of Zhang et al. [11]. The authors consider formations of robots that receive absolute position measurements, as well as robot-to-robot measurements (i.e., relative range, bearing, or orientation). A study of the structure of the measurement equations shows that the information matrix corresponding to the exteroceptive measurements is a function of the relative positions of the robots, and a gradient-based optimization technique is employed to determine local maxima of the trace of this matrix. However, due to the non-concavity of the objective function, the selected optimization method does not guarantee global optimality of the solution. The effects of formation geometry in the case of *moving* robots is studied in [12]. In that work, an evolutionary optimization algorithm is proposed for determining the optimal relative positions of the robots in a moving formation. The optimality criterion is the steady-state position uncertainty of the team, and it is shown that genetic algorithm-based minimization is an appropriate tool for this problem, due to the existence of multiple local minima in the objective function. In [13], a robot team comprised of one master and two slave robots is considered, and a *portable landmarks-based* technique is adopted for localization, i.e., at each time instant at least one robot remains stationary. The authors propose a method for determining the optimal relative positions between the robots, and identify configurations that yield the maximum possible localization accuracy at the end of a straight-line path.

We note that in all aforementioned approaches the constraints imposed by the available computational and communication resources are not taken into consideration. In [14], particle filtering-based localization with limited processing power is examined. The authors study the case where, due to restricted CPU capabilities, $k > 1$ measurements become available in the time interval necessary to update the entire particle set. In an effort to avoid completely discarding these measurements, an approximate real-time particle filter is proposed, that expresses the belief function of the robot pose as a mixture of k belief functions. The sample set is separated in k subsets, and each of the measurements is employed to process one subset. This approach is well-suited for single-robot localization, where the dimension of the state vector is small, and localization is possible with a relatively small number of particles.

Our work is more closely related to work in the Sensor Networks community, that aims at determining the optimal scheduling of measurements received by a *static* set of sensors, in order to attain the best possible estimation results. Representative examples of this line of research can be found in [15], [16], [17], while a similar analysis, in the context of designing observers for dynamical systems, is presented in [18], [19], [20], [21]. The defining assumption in all these cases is that the observation model switches *sequentially* between modes determined by the candidate *subsets* of sensors, a *finite* number of times during a certain time interval. This problem amounts to determining the optimal measurement ordering, so as to maximize the achieved estimation accuracy and/or minimize the consumed energy [17]. For this problem, tree-search algorithms (e.g., [15], [16]), as well as optimization methods in the continuous domain (e.g., [18]-[21]), have been proposed.

The main limitation of these approaches, that consider a *finite* time-horizon (or equivalently a finite number of measurements), is that the complexity of determining the optimal sensing strategy increases, often exponentially (e.g., in tree-search based algorithms) as the time-span of sensor operation increases. In contrast, in our work we consider the *frequencies* of the measurements as the design variables, and we are interested in the *steady-state* estimation accuracy. The benefit of this formulation is that the optimal strategy has to be determined only *once*, potentially off-line, for a given spatial configuration of the sensors, and the computational cost of determining the optimal solution is *independent* of the time duration of the sensor's operation.

A formulation of the scheduling problem that also considers the infinite time-horizon problem has been presented in [22], [23]. In that work, a probability density function (pdf) is employed to describe the time instants at which each measurement is performed. An upper bound on the *expected steady-state covariance* of the target's position estimate is then computed as a function of the pdf's parameters. Employing a numerical optimization routine, it is possible to minimize this upper bound, and the resulting pdf is used as the optimal sensing strategy. Despite its mathematical elegance, this approach only aims at optimizing an upper bound (this is the

case also in [20]). Since no means of determining the looseness of the bound are available, we cannot have any guarantee of optimality, or a measure of suboptimality, when this method is used.

Our work differs from the aforementioned approaches, in that we consider a team of robots that *move* while maintaining their formation, and localize in a global coordinate frame. The steady-state covariance matrix of the robots' localization is expressed as a function of the frequencies of all the exteroceptive measurements, and we seek to select the optimal frequencies, in order to attain the best possible positioning accuracy for the team. The constraints imposed by the available resources are taken into account, and their effect on the attainable localization accuracy is examined.

III. Problem Formulation

We consider a team of N robots that move in formation, employing a suitable control strategy in order to maintain a constant heading and constant relative positions among them. The spatial configuration of the robots is assumed to be given, defined, for example, by the application at hand. All robots are equipped with proprioceptive sensors (such as wheel encoders) that measure their translational and rotational velocities at every time step. Additionally, some (or all) of the robots are equipped with exteroceptive sensors that enable them to measure: (i) distance between two robots, (ii) relative bearing between two robots, (iii) relative orientation between two robots, (iv) absolute position of a robot, and (v) absolute orientation of a robot. The measurements received from all the sensors are processed using an Extended Kalman Filter (EKF), in order to estimate the pose of the robots with respect to a *global* frame of reference.

Clearly, due to cost, reliability, or other design considerations, it may not be desirable for all robots to be equipped with identical sensors. This potential heterogeneity of the team is incorporated naturally in our approach, under the restriction that *at least one* robot has access, at least intermittently, to absolute position information, such as those provided by a GPS or from observing previously mapped features. This constraint is imposed because our goal is to minimize the *steady-state* localization uncertainty of the robots in a global coordinate frame. It is well known [24], [25], that when no absolute position information is available to a robot team, the system is unobservable, and at steady state, the uncertainty of the robots continuously increases. The assumption for the availability of absolute positioning information could be raised if we studied a scenario in which only *relative* localization was sought. For that scenario, robot-to-robot measurements would (under certain conditions) be sufficient, in order to attain a bounded steady-state error covariance, and our approach would be applicable.

Since the processing, communication, and power resources allocated for localization are inevitably limited, it may not be possible to process all available exteroceptive measurements at every time instant. In this paper, we assume that measurements can be processed at a maximum total rate of f_{total} throughout the robot team, and our goal is to determine the frequency at which *each individual sensor* should be utilized, in order to attain the highest possible localization accuracy. Before describing the details of our method for obtaining the optimal measurement frequencies, we now present the system and measurement models used for pose estimation.

A. Propagation

Consider N non-holonomic robots moving in 2D. The discrete-time kinematic equations for the i-th robot are:

$$x_i(k+1) = x_i(k) + V_i(k)\delta t \cos(\phi_i(k)) \quad (1)$$

$$y_i(k+1) = y_i(k) + V_i(k)\delta t \sin(\phi_i(k)) \quad (2)$$

$$\phi_i(k+1) = \phi_i(k) + \omega_i(k)\delta t, \quad i = 1 \ldots N \quad (3)$$

where $V_i(k)$ and $\omega_i(k)$ denote the translational and rotational velocity of the i-th robot at time step k, respectively, and δt is the odometry sampling period. In the Kalman filter framework, the position estimates of robot i are propagated using the measurements from its proprioceptive sensors:[1]

$$\hat{x}_{i_{k+1|k}} = \hat{x}_{i_{k|k}} + V_{m_i}(k)\delta t \cos(\hat{\phi}_{i_{k|k}}) \quad (4)$$

$$\hat{y}_{i_{k+1|k}} = \hat{y}_{i_{k|k}} + V_{m_i}(k)\delta t \sin(\hat{\phi}_{i_{k|k}}) \quad (5)$$

$$\hat{\phi}_{i_{k+1|k}} = \hat{\phi}_{i_{k|k}} + \omega_{m_i}(k)\delta t, \quad i = 1 \ldots N \quad (6)$$

where $V_{m_i}(k)$ and $\omega_{m_i}(k)$ are the measurements of the robot's translational and rotational velocity, respectively. By linearizing Eqs. (1) - (3) the error propagation equation for the robot's pose is readily derived:

$$\begin{bmatrix} \widetilde{x}_{i_{k+1|k}} \\ \widetilde{y}_{i_{k+1|k}} \\ \widetilde{\phi}_{i_{k+1|k}} \end{bmatrix} = \begin{bmatrix} 1 & 0 & -V_{m_i}(k)\delta t \sin(\hat{\phi}_{i_{k|k}}) \\ 0 & 1 & V_{m_i}(k)\delta t \cos(\hat{\phi}_{i_{k|k}}) \\ 0 & 0 & 1 \end{bmatrix} \begin{bmatrix} \widetilde{x}_{i_{k|k}} \\ \widetilde{y}_{i_{k|k}} \\ \widetilde{\phi}_{i_{k|k}} \end{bmatrix} + \begin{bmatrix} \delta t \cos(\hat{\phi}_{i_{k|k}}) & 0 \\ \delta t \sin(\hat{\phi}_{i_{k|k}}) & 0 \\ 0 & \delta t \end{bmatrix} \begin{bmatrix} w_{V_i}(k) \\ w_{\omega_i}(k) \end{bmatrix}$$

$$\Leftrightarrow \quad \widetilde{X}_{i_{k+1|k}} = \Phi_i(k)\widetilde{X}_{i_{k|k}} + G_i(k)W_i(k) \quad (7)$$

where $w_{V_i}(k)$ and $w_{\omega_i}(k)$ are white, zero-mean, Gaussian and uncorrelated noise sequences of variance $\sigma^2_{V_i}$ and $\sigma^2_{\omega_i}$ affecting the linear and rotational velocity measurements, respectively.

Considering that the robot team moves in a predefined formation, all robots are required to head towards the same direction, and move with the same velocity, both of which are known constants. Assuming that a motion controller is used in order to minimize the deviations from the desired formation, and that the accuracy of the velocity measurements and orientation estimates is sufficiently high, we can replace the quantities $V_{m_i}(k)$, $\omega_{m_i}(k)$, and $\hat{\phi}_{i_{k|k}}$ in the above expressions by their respective predefined values, V_o, ω_o and ϕ_o. Thus the time-varying matrices $\Phi_i(k)$ and $G_i(k)$ can be approximated

[1] In the remainder of the paper the subscript $\ell|j$ refers to the estimate of a quantity at time step ℓ, after all measurements up to time-step j have been processed. The "hat" symbol, $\widehat{\ }$, is used to denote the estimated value of a quantity, while the "tilde" symbol, $\widetilde{\ }$, is used to signify the error between the actual value of a quantity and its estimate. The relationship between a variable, x, and its estimate, $\widehat{x}$, is $\widetilde{x} = x - \widehat{x}$.

by the *constant* matrices:

$$\Phi_i(k) \simeq \begin{bmatrix} 1 & 0 & -V_o\delta t\sin(\phi_o) \\ 0 & 1 & V_o\delta t\cos(\phi_o) \\ 0 & 0 & 1 \end{bmatrix} = \Phi_o \quad (8)$$

and

$$G_i(k) \simeq \begin{bmatrix} \delta t\cos(\phi_o) & 0 \\ \delta t\sin(\phi_o) & 0 \\ 0 & \delta t \end{bmatrix} = G_o \quad (9)$$

With this approximation, the error-state covariance propagation equation for the i-th robot can be written as:

$$P_{i_{k+1|k+1}} = \Phi_o P_{i_{k+1|k}} \Phi_o^T + G_o Q_i G_o^T \quad (10)$$

where $Q_i = \mathrm{diag}(\sigma_{V_i}^2, \sigma_{\omega_i}^2)$.

At this point, a comment regarding our selection of the state propagation model is due. In the preceding expressions, a simple non-holonomic kinematic model for the robots' motion is employed, because it is appropriate for the robots used in our experiments (cf. Section VI). However, *any* other motion model could be employed in our analysis, such as that of skid-steered vehicles [26], that of four-wheeled vehicles [3], or a more accurate kinematic model that assumes constant rotational velocity during an integration step [27]. If a different motion model is used, the structure of the Jacobians (cf. Eqs. (8) and (9)) will be different, but the approach for determining the optimal measurement frequencies remains unchanged.

The state vector for the entire robot team, $\mathbf{X}$, is defined as the $3N \times 1$ vector comprising of the poses of all the robots, $X_i = [x_i \;\; y_i \;\; \phi_i]^T,\ i = 1 \ldots N$. Therefore, the covariance propagation equation can be written as:

$$\mathbf{P}_{k+1|k} = \mathbf{\Phi}\mathbf{P}_{k|k}\mathbf{\Phi}^T + \mathbf{Q} \quad (11)$$

where $\mathbf{P}_{\ell|k} = E\{\widetilde{\mathbf{X}}_{\ell|k}\widetilde{\mathbf{X}}_{\ell|k}^T\}$, $\mathbf{\Phi} = \mathbf{Diag}(\Phi_o)$, and $\mathbf{Q} = \mathbf{Diag}(G_o Q_i G_o^T)$ are $3N \times 3N$ block-diagonal matrices.

B. Update

The robots of the team employ the measurements recorded by their exteroceptive sensors, in order to perform pose updates in the EKF. The i-th exteroceptive measurement is described by the (generally nonlinear) model

$$z_i(k) = h(\mathbf{X}(k), n_i(k)) \quad (12)$$

where $n_i(k)$ is a Gaussian noise vector. In the EKF framework, we employ linearization, to obtain the measurement error equation

$$\widetilde{z}_i(k) = H_i(k)\widetilde{\mathbf{X}}(k) + \Gamma_i(k) n_i(k) \quad (13)$$

where

$$H_i(k) = \nabla_{\mathbf{X}(k)} h(\mathbf{X}(k), n_i(k))\Big|_{\widehat{\mathbf{X}}(k),0} \quad (14)$$

and

$$\Gamma_i(k) = \nabla_{n_i(k)} h(\mathbf{X}(k), n_i(k))\Big|_{\widehat{\mathbf{X}}(k),0} \quad (15)$$

Clearly, the Jacobian matrices $H_i(k)$ and $\Gamma_i(k)$ are time-varying, due to the dependence on the state estimates. For many practical observation models, the Jacobians are only functions of the robots' orientation and the relative poses between robots, both of which are, in the case of formation motion, approximately constant. We can thus employ the *constant* approximations

$$H_i(k) \simeq \nabla_{\mathbf{X}(k)} h(\mathbf{X}(k), n_i(k))\Big|_{\mathbf{X}_o(k),0} = H_{i_o} \quad (16)$$

and

$$\Gamma_i(k) \simeq \nabla_{n_i(k)} h(\mathbf{X}(k), n_i(k))\Big|_{\mathbf{X}_o(k),0} = \Gamma_{i_o} \quad (17)$$

where $\mathbf{X}_o(k)$ is the desired state of the formation at time step k. To demonstrate the application of our method based on concrete examples, we hereafter consider five types of exteroceptive measurements:

1) Relative range measurements: If robot i is equipped with a sensor capable of measuring the distance of other robots with respect to itself, such as a laser scanner, then the distance measurement between robots i and j is:

$$z_{\rho_{ij}}(k) = \sqrt{\Delta x_{ij}(k)^2 + \Delta y_{ij}(k)^2} + n_{\rho_{ij}}(k) \quad (18)$$

where $\Delta x_{ij} = x_j - x_i$, $\Delta y_{ij} = y_j - y_i$, and $n_{\rho_{ij}}$ is a white, zero-mean, Gaussian noise process, whose standard deviation, σ_{ρ_i}, is determined by the characteristics of the sensor. By linearizing, the measurement error equation is determined:[2]

$$\begin{aligned} \widetilde{z}_{\rho_{ij}}(k) &= H_{\rho_{ij}}(k)\widetilde{\mathbf{X}}(k) + n_{\rho_{ij}}(k) \\ &= \begin{bmatrix} 0 & .. & H_{\rho_i} & .. & H_{\rho_j} & .. & 0 \end{bmatrix} \widetilde{\mathbf{X}} + n_{\rho_{ij}} \end{aligned} \quad (19)$$

where $H_{\rho_{ij}}(k)$ is a $1 \times 3N$ matrix, whose i-th and j-th block elements are, respectively:

$$H_{\rho_j}(k) = -H_{\rho_i}(k) = \begin{bmatrix} \frac{\widehat{\Delta x}_{ij}(k)}{\hat{\rho}_{ij}(k)} & \frac{\widehat{\Delta y}_{ij}(k)}{\hat{\rho}_{ij}(k)} & 0 \end{bmatrix} \quad (20)$$

In the preceding expression, $\widehat{\Delta x}_{ij}(k)$, $\widehat{\Delta y}_{ij}(k)$ and $\hat{\rho}_{ij}(k)$ represent the estimated differences in the x and y coordinates, and the estimated distance between robots i and j, respectively. By replacing the estimates with the values corresponding to the desired formation of the robots, we can derive the following approximations:

$$H_{\rho_i}(k) \simeq \begin{bmatrix} \frac{-\Delta x_{ij_o}}{\rho_{ij_o}} & \frac{-\Delta y_{ij_o}}{\rho_{ij_o}} & 0 \end{bmatrix} = H_{\rho_{i_o}} \quad (21)$$

$$H_{\rho_j}(k) \simeq \begin{bmatrix} \frac{\Delta x_{ij_o}}{\rho_{ij_o}} & \frac{\Delta y_{ij_o}}{\rho_{ij_o}} & 0 \end{bmatrix} = H_{\rho_{j_o}} \quad (22)$$

For practical reasons, it may not be possible for all robots to measure relative distances to all other robots in the team. For example, some robots may not be equipped with range sensors, or certain measurements may be impossible due to occlusions in the formation. In order to describe the set of all possible measurements we define the set

$$\mathcal{H}_\rho = \{H_{\rho_{ij}} |\ \text{robot } i \text{ can measure range to robot } j\}$$

[2]In the following derivations, the time step indices are omitted wherever this does not cause confusion. This is done in order to make the notation less cumbersome.

2) Relative bearing measurements: Assuming robot i measures the relative bearing towards robot j, the corresponding measurement equation is:

$$z_{\theta_{ij}}(k) = \text{Atan2}(\Delta y_{ij}(k), \Delta x_{ij}(k)) - \phi_i(k) + n_{\theta_{ij}}(k) \quad (23)$$

where $n_{\theta_{ij}}(k)$ is a white, zero-mean, Gaussian noise process, with standard deviation σ_{θ_i}. Linearization yields the following measurement error equation:

$$\begin{aligned}\widetilde{z}_{\theta_{ij}}(k) &= H_{\theta_{ij}}(k)\widetilde{\mathbf{X}}(k) + n_{\theta_{ij}}(k) \\ &\simeq H_{\theta_{ij_o}}\widetilde{\mathbf{X}}(k) + n_{\theta_{ij}}(k) \\ &= \begin{bmatrix} 0 & .. & H_{\theta_{i_o}} & .. & H_{\theta_{j_o}} & .. & 0 \end{bmatrix}\widetilde{\mathbf{X}} + n_{\theta_{ij}} \quad (24)\end{aligned}$$

where we have once again approximated the time-varying position estimates with their constant, desired values. Note that $H_{\theta_{ij_o}}$ is a $1 \times 3N$ matrix, whose i-th and j-th block elements are, respectively:

$$H_{\theta_{i_o}} = \begin{bmatrix} \frac{\Delta y_{ij_o}}{\rho^2_{ij_o}} & \frac{-\Delta x_{ij_o}}{\rho^2_{ij_o}} & -1 \end{bmatrix} \quad (25)$$

$$H_{\theta_{j_o}} = \begin{bmatrix} \frac{-\Delta y_{ij_o}}{\rho^2_{ij_o}} & \frac{\Delta x_{ij_o}}{\rho^2_{ij_o}} & 0 \end{bmatrix} \quad (26)$$

Similarly to the case of range measurements, we describe all possible bearing measurements with the set

$$\mathcal{H}_\theta = \{H_{\theta_{ij}} | \text{ robot } i \text{ can measure bearing to robot } j\}$$

3) Relative orientation measurements: If robot i measures the relative orientation of robot j, the corresponding measurement equation is:

$$z_{\Delta\phi_{ij}}(k) = \phi_j(k) - \phi_i(k) + n_{\Delta\phi_{ij}}(k) \quad (27)$$

where $n_{\Delta\phi_{ij}}(k)$ is a white, zero-mean, Gaussian noise process, with standard deviation $\sigma_{\Delta\phi_i}$. The measurement error equation is:

$$\begin{aligned}\widetilde{z}_{\Delta\phi_{ij}}(k) &= H_{\Delta\phi_{ij}}\widetilde{\mathbf{X}} + n_{\Delta\phi_{ij}}(k) \\ &= \begin{bmatrix} .. & \underbrace{[0\ 0\ -1]}_{i\text{th block}} & .. & \underbrace{[0\ 0\ 1]}_{j\text{th block}} & .. \end{bmatrix}\widetilde{\mathbf{X}} + n_{\Delta\phi_{ij}}(k)\end{aligned}$$

All possible relative orientation measurements are described by the set

$$\mathcal{H}_{\Delta\phi} = \{H_{\Delta\phi_{ij}} | \text{ robot } i \text{ can measure rel. ori. of robot } j\}$$

4) Absolute orientation measurements: If the i-the robot of the team is equipped with an absolute orientation sensor, such as a compass, the corresponding measurement equation is:

$$z_{\phi_i}(k) = \phi_i(k) + n_{\phi_i}(k) \quad (28)$$

where n_{ϕ_i} is a white, zero-mean, Gaussian noise process, with standard deviation σ_{ϕ_i}. In this case the measurement error equation is:

$$\begin{aligned}\widetilde{z}_{\phi_i}(k) &= H_{\phi_i}\widetilde{\mathbf{X}}(k) + n_{\phi_i}(k) \\ &= \begin{bmatrix} 0 & .. & \underbrace{[0\ \ 0\ \ 1]}_{i\text{th block}} & .. & 0 \end{bmatrix}\widetilde{\mathbf{X}}(k) + n_{\phi_i}(k) \quad (29)\end{aligned}$$

All possible absolute orientation measurements are described by the set

$$\mathcal{H}_\phi = \{\phi_i | \text{ robot } i \text{ can measure absolute orientation}\}$$

5) Absolute position measurements: In this work, the robots localize with respect to a global coordinate frame. Therefore, in order for the position errors to remain bounded for all times, it is necessary that at least one of the robots has access to absolute position measurements. The measurement equation for the i-the robot is

$$z_{p_i}(k) = \begin{bmatrix} x_i(k) & y_i(k) \end{bmatrix}^T + n_{p_i}(k) \quad (30)$$

where $n_{p_i}(k)$ is a 2×1 white, zero-mean, Gaussian noise process, with covariance matrix R_{p_i}. The measurement error equation for this type of measurement is

$$\begin{aligned}\widetilde{z}_{p_i}(k) &= H_{p_i}\widetilde{\mathbf{X}}(k) + n_{p_i}(k) \\ &= \begin{bmatrix} \mathbf{0}_{2\times 3} & .. & \underbrace{[I_2\ \ \mathbf{0}_{2\times 1}]}_{i\text{th block}} & .. & \mathbf{0}_{2\times 3} \end{bmatrix}\widetilde{\mathbf{X}}(k) + n_{p_i}(k)\end{aligned}$$

where H_{p_i} is a $2 \times 3N$ matrix, I_n denotes the $n \times n$ identity matrix, and $\mathbf{0}_{m\times n}$ is a $m \times n$ matrix of zeros.

In order to describe all possible absolute position measurements we define the set

$$\mathcal{H}_p = \{H_{p_i} | \text{ robot } i \text{ can measure absolute position}\}$$

C. The Riccati recursion

The exteroceptive measurements recorded by the robots at each time instant are processed by the EKF, in order to update the robots' pose estimates. The covariance update equation of the EKF is

$$\mathbf{P}_{k+1|k+1} = \mathbf{P}_{k+1|k} - \mathbf{P}_{k+1|k}\mathbf{H}_k^T\mathbf{S}_k^{-1}\mathbf{H}_k\mathbf{P}_{k+1|k} \quad (31)$$

where $\mathbf{S}_k = \mathbf{H}_k\mathbf{P}_{k+1|k}\mathbf{H}_k^T + \mathbf{R}_k$. In these equations $\mathbf{H}_k$ is the measurement matrix for the system at time step k, and $\mathbf{R}_k$ is the corresponding measurement-noise covariance matrix.

In most realistic cases, when only a subset of sensor measurements, often varying, can be processed at each time instant, $\mathbf{H}_k$ and $\mathbf{R}_k$ will not remain constant, and will possibly vary even in size at each time step. Specifically, if at time step k a total of m_k measurements are performed, $\mathbf{H}_k$ will comprise m_k block rows belonging in the set $\mathcal{H} = \mathcal{H}_\rho \bigcup \mathcal{H}_\theta \bigcup \mathcal{H}_{\Delta\phi} \bigcup \mathcal{H}_\phi \bigcup \mathcal{H}_p$, and $\mathbf{R}_k$ will be a block-diagonal matrix whose elements can be defined accordingly.

Combining Eqs. (11) and (31) yields the Riccati recursion [28]

$$\begin{aligned}\mathbf{P}_{k+2|k+1} = \ &\mathbf{\Phi}\left(\mathbf{P}_{k+1|k} - \mathbf{P}_{k+1|k}\mathbf{H}_k^T\mathbf{S}_k^{-1}\mathbf{H}_k\mathbf{P}_{k+1|k}\right)\mathbf{\Phi}^T \\ &+ \mathbf{Q} \quad (32)\end{aligned}$$

that describes the discrete-time evolution of the covariance of the pose estimates for the robot team. If the system is observable, then after undergoing an initial, transient phase, the covariance matrix will enter a steady state, where its elements will fluctuate around some mean value (cf. Fig. 1). Had we been able to provide a description of this mean value as a function of the measurement frequencies, then we would have a means of directly relating the localization performance of the system to these frequencies. However, there exist no analytical tools for describing the mean value of a Riccati recursion with time-varying coefficients. To solve this problem, we propose a transition from the discrete-time system model to a continuous-time one, as described in the following section.

IV. The Riccati differential equation

In this section, we present the main idea of this paper, which enables us to formulate a convex optimization problem for determining the optimal frequencies at which the measurements of the available sensors should be utilized. Intuitively, the rate at which a given sensor is providing measurements determines the amount of localization information this sensor contributes per unit of time. If we view this as a *continuous information flow*, then the frequency of the measurements determines the *magnitude* of the flow. This key idea allows us to express the steady-state localization accuracy of the robots as an analytical function of the measurement frequencies, by employing a transition to the continuous-time domain.

In particular, in [28] it is shown that given a discrete-time Riccati recursion, we can derive a continuous-time Riccati differential equation that is *equivalent*, in the sense that the state estimates' accuracy in both cases is the same. Specifically, if state observations whose covariance is R_d are performed with frequency f in the discrete-time description, then the equivalent continuous-time measurements' covariance function is $E\{n_c(t)n_c^T(\tau)\} = R_c\delta(t-\tau)$, where $n_c(\cdot)$ is a white Gaussian noise process, $\delta(\cdot)$ denotes the Dirac delta function, and[3] $R_c = f^{-1}R_d$. We observe that the covariance matrix of the continuous-time model is scaled by the inverse measurement frequency, to ensure a constant information influx. By a similar argument, we can derive the appropriate value of the system noise covariance matrix.

We now employ the idea of deriving an equivalent continuous-time Riccati, in order to formulate a *constant coefficient* differential equation for the covariance of the pose estimates in the robot team. Specifically, since each of the measurements in the set $\mathcal{H}$ occurs at a constant frequency (generally different for each measurement), we can formulate a continuous-time model, where *all* the measurements occur continuously, and the covariance of each measurement is scaled by the inverse of its frequency. In the continuous-time formulation, the measurement matrix $\mathbf{H}_c$ will be a *constant* matrix comprising of all the block rows in the set $\mathcal{H}$. The covariance matrix of the measurements, $\mathbf{R}_c$, will be a (block) diagonal matrix, with elements the *weighted* covariances of the discrete-time measurements. For example, if robot i receives absolute orientation measurements with covariance σ_{ϕ_i} at a rate of f_{ϕ_i}, then the continuous-time covariance function corresponding to this measurement is $R_{\phi_{i_c}}\delta(t-\tau)$, where

$$R_{\phi_{i_c}} = \sigma^2_{\phi_{i_c}} = \frac{\sigma^2_{\phi_{i_d}}}{f_{\phi_i}} = \frac{1}{f_{\phi_i}}R_{\phi_{i_d}} \tag{33}$$

We can now use the Riccati differential equation in order to describe the time evolution of the covariance of the robots' pose estimates. We note that the state transition matrix for the system in continuous time is equal to $\mathbf{F}_c = \mathbf{Diag}(F_o)$, where

$$F_o = \begin{bmatrix} 0 & 0 & -V_o\sin(\phi_o) \\ 0 & 0 & V_o\cos(\phi_o) \\ 0 & 0 & 0 \end{bmatrix} \tag{34}$$

[3]The subscripts c and d denote continuous- and discrete-time quantities, respectively.

while the matrix describing the influx of uncertainty in the continuous-time system is equal to $\mathbf{Q}_c = \mathbf{Diag}(G_{o_c}Q_{i_c}G_{o_c}^T)$ with

$$G_{o_c} = \begin{bmatrix} \cos(\phi_o) & 0 \\ \sin(\phi_o) & 0 \\ 0 & 1 \end{bmatrix} \tag{35}$$

and $Q_{i_c} = f_{o_i}^{-1}\,\mathrm{diag}(\sigma^2_{V_i}, \sigma^2_{\omega_i})$. In this last expression, f_{o_i} denotes the rate at which robot i samples its proprioceptive sensors. Using the previous relations, the Riccati differential equation is written as

$$\dot{\mathbf{P}}(t) \;=\; \mathbf{F}_c\mathbf{P}(t) + \mathbf{P}(t)\mathbf{F}_c^T + \mathbf{Q}_c - \mathbf{P}(t)\mathbf{C}\mathbf{P}(t) \tag{36}$$

where we have denoted

$$\mathbf{C} \;=\; \mathbf{H}_c^T\mathbf{R}_c^{-1}\mathbf{H}_c \tag{37}$$

The first two terms in Eq. (36) describe the effect of the dynamics of the system on the state covariance matrix, the term $\mathbf{Q}_c$ accounts for the *increase in uncertainty* due to the existence of system noise, while the term $\mathbf{P}(t)\mathbf{C}\mathbf{P}(t)$ describes the *influx of localization information* due to the exteroceptive measurements. If we denote by M the total number of available exteroceptive measurements (i.e., the number of elements in $\mathcal{H}$), by f_i the frequency of the i-th measurement in $\mathcal{H}$, by H_i the corresponding measurement matrix, and by R_{d_i} the associated covariance matrix, then $\mathbf{C}$ can be rewritten as

$$\mathbf{C} \;=\; \sum_{i=1}^{M} f_i H_i^T R_{d_i}^{-1} H_i \;=\; \sum_{i=1}^{M} f_i C_i \tag{38}$$

We can therefore see that the elements of $\mathbf{C}$ are *linear combinations* of the measurement frequencies. This is an important observation, because it allows us to express the problem of determining the optimal measurement frequencies as a convex optimization problem, as shown in the next section.

We note that the Riccati equation in (36) is a *constant-coefficient* differential equation, and its steady-state solution, $\mathbf{P}_{ss}$, can be found by solving the Algebraic Riccati Equation (ARE)

$$\mathbf{F}_c\mathbf{P}_{ss} + \mathbf{P}_{ss}\mathbf{F}_c^T + \mathbf{Q}_c - \mathbf{P}_{ss}\mathbf{C}\mathbf{P}_{ss} = \mathbf{0} \tag{39}$$

The solution is a function of the matrix coefficients of the ARE [29], and therefore the steady-state covariance of the pose estimates for the robots of the formation is a *function of the measurement frequencies*, which appear in $\mathbf{C}$. To be more precise, $\mathbf{P}_{ss}$ is the steady-state covariance of the equivalent continuous-time system, whose parameters depend on the measurement frequencies. In Fig. 1, we present the time-evolution of the diagonal elements of the covariance matrix in the *actual* discrete-time system (solid lines) and compare them to the theoretical continuous-time computed values (dashed lines) computed by solving Eq. (39). For these simulations, a team of 3 robots, that have access to all four types of exteroceptive measurements, discussed in Section III-B, was considered. The relative positions, as well as the measurement frequencies for all robots were selected randomly.

It becomes clear that, at steady state, the actual values of the covariance fluctuate around the theoretically predicted values.

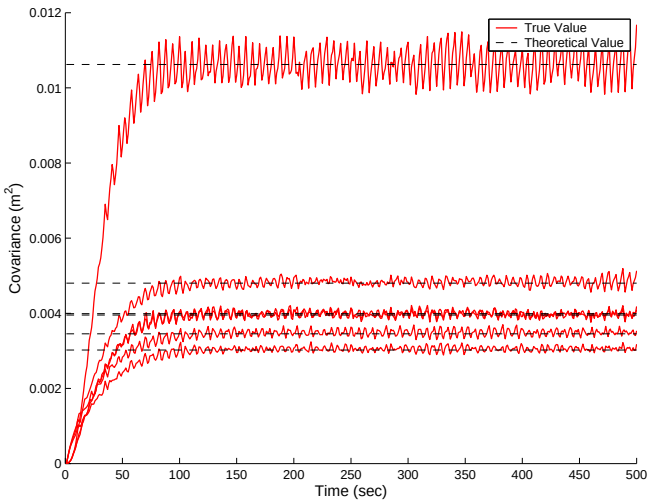

Fig. 1. True covariance vs. theoretical values. The diagonal elements of the covariance matrix corresponding to the position of the 3 robots are plotted.

Thus, we can employ the continuous-time analysis in order to study the properties of the localization accuracy in the formation.

V. Measurement Frequency Optimization

In this section, we formulate the problem of determining the optimal measurement frequencies as a convex optimization problem. Our goal is to determine the optimal frequencies for all available measurements, i.e., these frequencies that will yield the best possible localization results under given constraints. Clearly, in order to improve the localization accuracy of the formation, the steady-state covariance matrix should be minimized. However, $\mathbf{P}_{ss}$ is a $3N \times 3N$ matrix, and several criteria of optimality can be defined based on it (e.g., its determinant, its maximum eigenvalue, its trace). A difficulty that arises is that while the elements of $\mathbf{P}_{ss}$ that correspond to the position estimates of the robots have units of m^2, the elements that correspond to orientation have units of rad^2. Clearly, we cannot treat these two types of elements equally. One approach is to introduce a weighting matrix $\mathbf{W}$, and try to minimize a function of the weighted matrix $\mathbf{W}\mathbf{P}_{ss}\mathbf{W}^T$. However, any selection of $\mathbf{W}$ that would incorporate both the orientation and the position uncertainty in the objective function would be *ad-hoc* and thus difficult to motivate. We have therefore selected to focus only on the diagonal elements of $\mathbf{P}_{ss}$ that correspond to the position estimates of the robots, while ensuring that the orientation uncertainty of each robot does not exceed a threshold ϵ_ϕ (this is necessary, in order to guarantee small linearization errors). We thus formulate the following optimization problem:

$$\begin{aligned} \textbf{minimize} \quad & \text{trace}(\mathbf{W}_p \mathbf{P}_{ss} \mathbf{W}_p^T) \\ \textbf{subject to} \quad & \mathbf{F}_c \mathbf{P}_{ss} + \mathbf{P}_{ss} \mathbf{F}_c^T + \mathbf{Q}_c - \mathbf{P}_{ss} \mathbf{C} \mathbf{P}_{ss} = \mathbf{0} \\ & \mathbf{C} = \sum_{i=1}^{M} f_i C_i \\ & 0 \leq f_i \leq f_{i_{\max}}, \text{for } i = 1 \ldots M \end{aligned} \tag{40}$$

$$\sum_{i=1}^{M} f_i \leq f_{\text{total}}$$

$$e_{3i}^T \mathbf{P}_{ss} e_{3i} \leq \epsilon_\phi, i = 1 \ldots N$$

In the preceding expressions e_i denotes the i-th canonical basis vector in the $3N$-dimensional space, and the weighting matrix is defined as

$$\mathbf{W}_p = \sum_{i=1}^{N} \left(e_{3i-2} e_{3i-2}^T + e_{3i-1} e_{3i-1}^T \right) \tag{41}$$

This definition means that the objective function is the sum of all the diagonal elements of $\mathbf{P}_{ss}$ that correspond to the positions of the robots. The linear constraints on the measurement frequencies express the facts that: (i) each sensor has a maximum sampling rate, $f_{i_{\max}}$, that cannot be exceeded, and (ii) the total frequency of the measurements cannot exceed a threshold, f_{total}, which is determined by the available communication and computational resources. We note that more general constraints can be incorporated in this formulation. For example, different types of measurements may have different costs associated with them, and this can be easily taken into consideration, by introducing weights for each of their frequencies. Additionally, if the positioning accuracy of some robots in the team is of higher importance than that of others, this can be easily taken into account by introducing weights, i.e., by defining a weighting matrix of the form

$$\mathbf{W}_{wp} = \sum_{i=1}^{N} w_i \left(e_{3i-2} e_{3i-2}^T + e_{3i-1} e_{3i-1}^T \right) \tag{42}$$

For clarity of presentation, the case of equal weights for all robots and all frequencies will be considered in the remainder of the paper.

In [30], it is shown that the steady-state solution of the ARE in Eq. (39) is a *convex* function of the matrix $\mathbf{C}$. Because the elements of $\mathbf{C}$ are linear functions of the measurement frequencies (cf. Eq. (38)), we conclude that $\mathbf{P}_{ss}$ is a *convex function of the measurement frequencies*. As a result, the optimization problem (40) is a convex one (the objective is a convex function, and the feasible set is convex). This is a very important property, because it guarantees that the problem has a unique global minimum which can be found using standard gradient-based optimization techniques [31].

Our initial approach to solving the optimization problem (40) was to employ an iterative gradient-based constrained-optimization method, in which at every iteration an instance of the ARE is solved to provide $\mathbf{P}_{ss}$ [32]. The method we used for solving the ARE was the one based on the Hamiltonian matrix [29]. Despite the simplicity of this approach, the numerical experiments we conducted indicated that due to ill-conditioning of the Hamiltonian matrix in cases where the total frequency of measurements is low, the ARE solver was often unable to provide a solution with sufficient accuracy. This caused the optimization procedure to suffer from a slow convergence rate, and to produce inaccurate results. Additionally, enforcing the constraints $e_{3i}^T \mathbf{P}_{ss} e_{3i} \leq \epsilon_\phi, i = 1 \ldots N$ in (40) had to be implemented in an *ad-hoc*

manner, by introducing an additional cost term in the objective, to penalize solutions with large orientation uncertainties.

In order to overcome the numerical problems and treat the constraints on the orientation uncertainty in a more elegant way, we reformulate the optimization problem as a Semi-Definite Programming (SDP) problem, which exhibits substantially better numerical characteristics. In particular, the following Lemma holds:

Lemma 1: The original problem in (40) is equivalent to the following one:

$$\begin{aligned}
\textbf{minimize} \quad & \mathrm{trace}(\mathbf{W}_p \mathcal{P} \mathbf{W}_p^T) \\
\textbf{subject to} \quad & \begin{bmatrix} \mathcal{P} & I_{3N} \\ I_{3N} & \mathbf{J} \end{bmatrix} \succeq \mathbf{0} \\
& \begin{bmatrix} -\mathbf{J}\mathbf{F}_c - \mathbf{F}_c^T\mathbf{J} + \sum_{i=1}^{M} f_i C_i & \mathbf{J}\mathbf{Q}_c^{1/2} \\ \mathbf{Q}_c^{1/2}\mathbf{J} & I_{3N} \end{bmatrix} \succeq \mathbf{0} \\
& 0 \leq f_i \leq f_{i_{\max}}, \text{for } i = 1 \ldots M \qquad (43) \\
& \sum_{i=1}^{M} f_i \leq f_{\text{total}} \\
& e_{3i}^T \mathcal{P} e_{3i} \leq \epsilon_\phi, i = 1 \ldots N
\end{aligned}$$

where the variables in this problem are the matrices $\mathcal{P}$ and $\mathbf{J}$, belonging to the positive semidefinite cone $\mathbf{S}_+^{3N}$, and the measurement frequencies, f_i, $i = 1 \ldots M$. In the above expressions the symbol $\succeq$ denotes matrix inequality in the positive semidefinite sense, and $\mathbf{Q}_c^{1/2}$ is the symmetric matrix square root of $\mathbf{Q}_c$.

Proof:

We first note that by employing the properties of the Schur complement, the first inequality constraint in problem (43) is written as:

$$\mathcal{P} \succeq \mathbf{J}^{-1} \qquad (44)$$

while the second matrix inequality is equivalent to:

$$-\mathbf{J}\mathbf{F}_c - \mathbf{F}_c^T\mathbf{J} + \sum_{i=1}^{M} f_i C_i - \mathbf{J}\mathbf{Q}_c\mathbf{J} \quad \succeq \quad \mathbf{0} \qquad (45)$$

Using these relations, problem (43) is written equivalently as

$$\begin{aligned}
\textbf{minimize} \quad & \mathrm{trace}(\mathbf{W}_p \mathcal{P} \mathbf{W}_p^T) \\
\textbf{subject to} \quad & \mathbf{J}^{-1} - \mathcal{P} \preceq \mathbf{0} \\
& \mathbf{J}\mathbf{F}_c + \mathbf{F}_c^T\mathbf{J} - \left(\sum_{i=1}^{M} f_i C_i \right) + \mathbf{J}\mathbf{Q}_c\mathbf{J} \preceq \mathbf{0} \\
& 0 \leq f_i \leq f_{i_{\max}}, \text{for } i = 1 \ldots M \qquad (46) \\
& \sum_{i=1}^{M} f_i \leq f_{\text{total}} \\
& e_{3i}^T \mathcal{P} e_{3i} \leq \epsilon_\phi, i = 1 \ldots N
\end{aligned}$$

This is a convex optimization problem, since the objective as well as the inequality constraints are convex. Our goal is to show that this problem is equivalent to the problem described in (40), in the sense that the optimal frequencies for this problem are also optimal for (40).

We observe that for *any* feasible point, Y, for (40), with $Y = (f_1, \ldots, f_M, \mathbf{P}_{ss}) \in \mathbb{R}^M \times \mathbf{S}_+^{3N}$, we can construct the point $\Xi = (f_1, \ldots, f_M, \mathcal{P} = \mathbf{P}_{ss}, \mathbf{J} = \mathbf{P}_{ss}^{-1}) \in \mathbb{R}^M \times \mathbf{S}_+^{3N} \times \mathbf{S}_+^{3N}$ which is also feasible for (46), and yields the *same* objective value.

Similarly, given any feasible point for the problem (46), we can also construct a feasible point for (40). Let $\Xi^\star = (f_1^\star, \ldots, f_M^\star, \mathcal{P}^\star, \mathbf{J}^\star)$ be the optimal solution to the problem (46). Then, solving the ARE

$$\mathbf{F}_c\mathbf{P}_{ss}^\star + \mathbf{P}_{ss}^\star\mathbf{F}_c^T + \mathbf{Q}_c - \mathbf{P}_{ss}^\star \left(\sum_{i=1}^{M} f_i^\star C_i \right) \mathbf{P}_{ss}^\star = \mathbf{0} \qquad (47)$$

for $\mathbf{P}_{ss}^\star$ yields a feasible point $Y^\star = (f_1^\star, \ldots, f_M^\star, \mathbf{P}_{ss}^\star)$ for the problem described in (40). In Appendix I it is shown that the objective value corresponding to $Y^\star$ in (40) is *equal* to the objective value corresponding to $\Xi^\star$ in (46). Using this key result, we can employ proof by contradiction to show that $Y^\star$ is optimal for (40). Specifically, if $Y^\star$ were not optimal, there would exist a point $\breve{Y}$ that would give an objective value smaller than that of $Y^\star$. But in that case, we would be able to construct a point $\breve{\Xi}$ for problem (46), that would give a smaller objective value than $\Xi^\star$. However, this is a contradiction since $\Xi^\star$ is optimal. Thus, the optimal solution for the measurement frequencies arising from problem (46) is also optimal for problem (40).

■

The above proof relies on the fact that the objective value corresponding to $Y^\star$ is equal to the optimal value of problem (46). To provide intuition about this key result, whose proof can be found in Appendix I, we consider the simple case where the weighting matrix $\mathbf{W}_p$ is replaced by the identity matrix, and thus the minimization objective in (46) is simply $\mathrm{trace}(\mathcal{P})$. We note that since $\mathcal{P}$ is bounded below *only* by $\mathbf{J}^{-1}$, selecting $\mathcal{P} = \mathbf{J}^{-1}$ yields the minimum cost. Thus, at the optimal solution we have $\mathcal{P}^\star = \mathbf{J}^{\star -1}$, and substitution in Eq. (45) yields

$$\mathbf{F}_c\mathcal{P}^\star + \mathcal{P}^\star\mathbf{F}_c^T + \mathbf{Q}_c - \mathcal{P}^\star \left(\sum_{i=1}^{M} f_i^\star C_i \right) \mathcal{P}^\star \preceq \mathbf{0} \qquad (48)$$

or equivalently,

$$\mathbf{F}_c\mathcal{P}^\star + \mathcal{P}^\star\mathbf{F}_c^T + \mathbf{Q}_c' - \mathcal{P}^\star \left(\sum_{i=1}^{M} f_i^\star C_i \right) \mathcal{P}^\star = \mathbf{0}, \quad \mathbf{Q}_c' \succeq \mathbf{Q}_c$$

Thus, $\mathcal{P}^\star$ satisfies an ARE with $\mathbf{Q}_c' \succeq \mathbf{Q}_c$. However, the solution of an ARE is a monotonically increasing function of $\mathbf{Q}_c$ [30], and therefore the smallest value of the objective function, $\mathrm{trace}(\mathcal{P})$, is obtained when $\mathbf{Q}_c'$ is minimum. Clearly, this occurs when $\mathbf{Q}_c' = \mathbf{Q}_c$, thus the optimal solution $\mathcal{P}^\star$ satisfies Eq. (48) with equality. Note that this ARE is *identical* to the one in Eq. (47), hence $\mathcal{P}^\star = \mathbf{P}_{ss}^\star$, which means that the objective values of the two problems are equal. We stress that this proof outline is only valid when $\mathbf{W}_p$ is invertible. This is clearly not the case for the selection of $\mathbf{W}_p$ in this paper (cf. Eq. (41)), and this results in a significantly more complicated proof in Appendix I. However, the main underlying ideas remain the same.

Notice that the solution of the SDP (43) does *not* involve explicitly solving an ARE, thus resulting in superior numerical performance. Additionally, by employing the principle of strong duality, which holds for convex SDPs under mild qualifications that are valid in the particular problem [31], we can obtain a bound for the suboptimality of any solution. In particular, for any convex SDP problem we can define a *dual* SDP maximization problem [31]. When strong duality holds, the optimal solutions to the primal and dual problems yield the same objective value. This implies that, if any solution to the dual problem of (43) is available, we immediately have a *lower bound* on the minimum attainable objective value for (43).

Most SDP solvers automatically generate the dual problem, and proceed by simultaneously solving the primal and dual problems in an iterative fashion. Therefore the problem of determining the optimal measurement frequencies is solved by an *any-time algorithm*, since at any point during the solution procedure, a suboptimal solution is available. Moreover, by comparing the objective value of this intermediate solution to that of the corresponding intermediate solution of the dual problem, and employing strong duality, we obtain a concrete measure of "how good" the solution is. In a scenario where a large number of sensors is involved, and in which computation time is a significant factor (e.g., if we are solving in real-time to determine the best sensing strategy in a slowly varying formation), we may wish to trade-off optimality for efficiency, and in this case, the any-time property of the solution algorithm is very important.

At this point, we comment on the applicability of the method to cases where the assumption of a constant formation shape does not hold. A significant property of the solution to the ARE in Eq. (39) is that it is *independent* of the initial conditions, since the system under consideration is observable. This implies that if the geometry of the robot formation changes temporarily, for example due to the presence of obstacles that need to be avoided, then, once the robots return to the initial configuration, the solution becomes valid again. For practical purposes, this observation means that if we know in advance that a robot team will move in a known formation *most of the time*, then it might be desirable, from an implementation point of view, to use the measurement frequencies obtained with the proposed method for the entire duration of the robots' run.

If alternatively, the optimal sequence of measurements for a time-varying formation were sought, a tree-search within a finite time horizon of n time steps would be necessary [22]. However, the complexity of such a search is exponential in the number of time-steps, and can become intractable even for a search within a short-time horizon, if many measurements are available in the system. Such a search would need to be performed necessarily in real time, employing the most current pose estimates for the robots, and the results would need to be transmitted to all the members of the team. Contrary to that, the proposed method lends itself to off-line execution[4], before the robot team is deployed, and additionally, programming the sensors to record measurements at fixed time intervals is simpler. Clearly, the proposed approach is suboptimal when the robots do not maintain a fixed formation, and its performance has to be evaluated on a case-by-case basis.

[4]If the geometry of the relative positions of the robots of a team changes slowly, then our algorithm can also be used on-line, to provide an approximate solution to the optimal measurement scheduling.

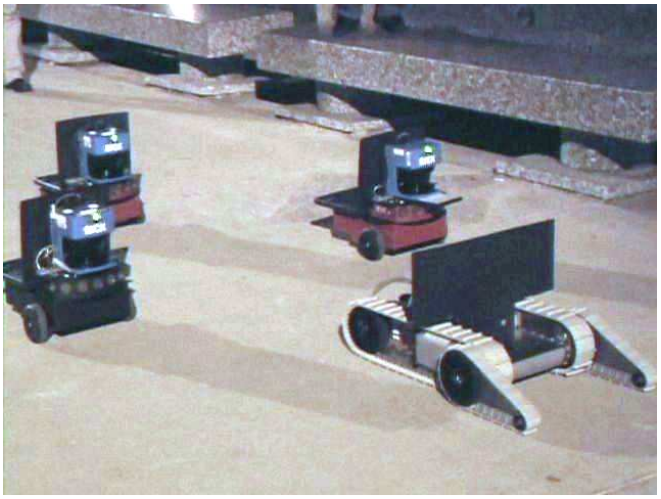

Fig. 2. The heterogeneous robot team used in our experiments.

VI. Experimental Results

To demonstrate the application of our method, we have conducted experiments with a heterogeneous robot team, comprised of one iRobot Packbot robot and 3 Pioneer-I robots. The robots move outdoors in a diamond-shaped formation, where the Packbot is the "leader", as shown in Fig. 2. Each of the Pioneers is equipped with a laser scanner, and is able to detect the robots of the team that lie within its field of view. Using a linefitting technique, we are able to extract relative position (i.e., range and bearing) as well as relative orientation information. It is important to note that since the same laser points are used in order to measure the relative position and relative orientation of a particular robot, these measurements are correlated, and must be treated as a single, vector-valued measurement.

In addition to the relative pose measurements, absolute position and orientation measurements are provided to the team by a GPS receiver and a magnetic compass, which are mounted on the Packbot. In total, 5 relative pose measurements (the robot in the rear is able to measure the relative pose of all other robots, while the ones on the sides can only detect the formation leader) and 2 absolute measurements (absolute position and orientation of the Packbot) are available. The absolute measurements are available at a maximum frequency of 1Hz, while the relative pose measurements are available at a maximum frequency of 3Hz. In Fig. 3, the geometry of the formation is shown, and the available relative pose measurements are presented by the dash-dotted arrows. R_1 is the Packbot, while R_2 - R_4 are the Pioneer robots, and M_{ij} denotes the measurement of the relative pose of robot j with respect to robot i. The formation moves on a 50m-long path parallel to the global x axis at a velocity of $V_o = 0.2$m/sec. During the experiments the robots keep records of the raw

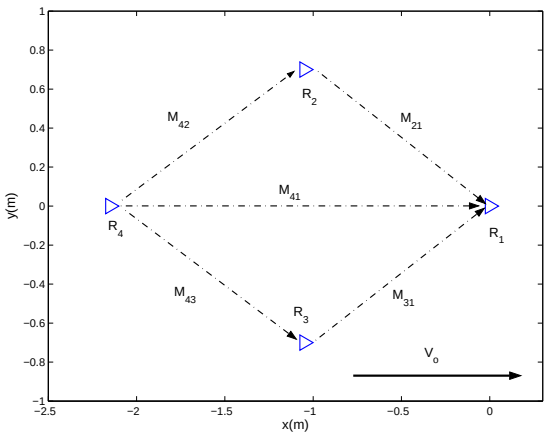

Fig. 3. Robot formation and motion direction. The dash-dotted arrows represent the relative pose measurements available to the robots.

sensor data, thus enabling us to run the EKF off-line with various measurement frequencies, and facilitating comparison between different sensing strategies.

In order to maintain the desired formation shape, a simple leader-follower control scheme is implemented. Each of the Pioneer-I robots adjusts its rotational and translational velocity using a PI-controller. The feedback input to the controller is the difference between the desired and the measured relative pose of the formation leader with respect to the measuring robot. Since control is performed locally on each robot, it does not introduce any communication overhead, and additionally, it is very inexpensive computationally. Although very simple, this controller is sufficient for the purposes of our experiments, in which the formation is commanded to move in an almost straight line. In fact, the deviations from the desired geometry, that arise due to the simple controller we have employed, facilitate the demonstration of the robustness of our measurement frequency optimization method to small changes in formation shape[5].

By constraining the maximum total frequency of measurements that can be processed by the system to be equal to 3Hz, the optimal frequencies of all measurements are shown in Table I. These results are obtained by a Matlab implementation of the algorithm, that requires 11secs of CPU time on a 1.6GHz Pentium M processor. In order to execute the optimization algorithm, it is necessary to evaluate the matrices C_i (cf. Eq. (38)). This was performed by computing the measurement covariance matrices as well as the Jacobians H_i for each of the exteroceptive measurements, based on the nominal formation geometry. From the numerical results in Table I, we note that the absolute position and absolute orientation sensors are utilized at their maximum frequency, while the remaining resources are allocated to the relative pose measurements. It is interesting to note that the measurement between the rear robot and the leader is assigned a smaller

[5]We should note that the objective of this work is the determination of optimal measurement frequencies given a formation geometry, and *not* the design of an optimal controller for maintaining such a desired geometry. This second problem has received considerable attention in the literature, and the interested reader is referred to [33] for an overview of existing approaches.

TABLE I

OPTIMAL MEASUREMENT FREQUENCIES FOR THE EXPERIMENT

GPS	Comp.	M_{21}	M_{42}	M_{41}	M_{43}	M_{31}
1.0	1.0	0.216	0.234	0.099	0.234	0.216

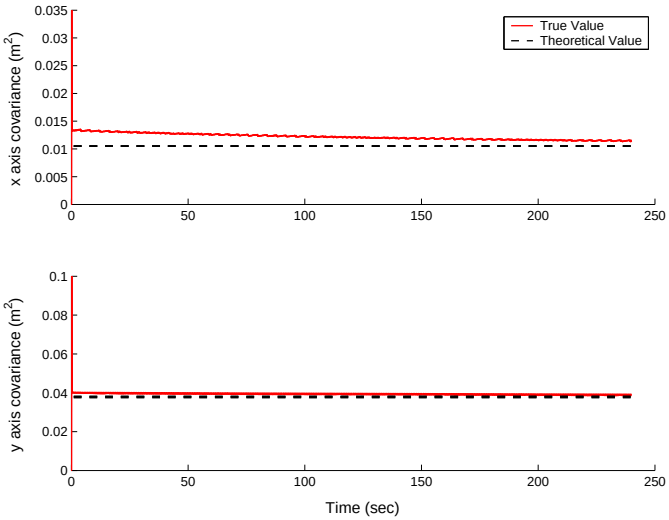

Fig. 4. Time evolution of the covariance along the two coordinate axes for all the robots, when the optimal measurement frequencies are used. The (red) solid lines represent the actual covariance values computed by the EKF, while the dashed lines represent the theoretically computed steady-state values.

frequency (although *not* zero), which should be attributed to the fact that this measurement is less accurate, due to the larger distance from the leader.

In Fig. 4 we present the time evolution of the covariance along the x and y axes, for the robots of the team (solid lines). The time evolution of the actual covariance is compared to the theoretically predicted values (dashed lines), computed by solving the SDP (43) . Although the time duration of the experiment did not allow for the covariance matrix to converge fully to its steady-state value, these figures indicate, that the deviation between the theoretically predicted values, and those computed by the EKF, is very small. This deviation is due to the facts that i) there is a small discretization error inherent in the transition between the continuous- and discrete-time system models [28], ii) in the EKF the *estimates* for the pose of the robots are employed to evaluate the measurement Jacobians, and these estimates are generally not precisely equal to the desired poses of the robots, iii) the laser scanners provide measurements at a frequency which is only *approximately* constant, and iv) the formation maintains the desired geometry within some error, determined from the controller's performance.

Variations in the formation geometry during the experiment are shown in Fig. 5, where we plot the estimated coordinates of the relative position of R_1 with respect to R_4, as a function of time. As evident, the estimates deviate significantly from their nominal values of $(\Delta x_{14}, \Delta y_{14}) = (2, 0)$m. These deviations are primarily due to the rough terrain that the robots move on, which often resulted in the Pioneers' caster wheels getting stuck. As a consequence of the fluctuations in the

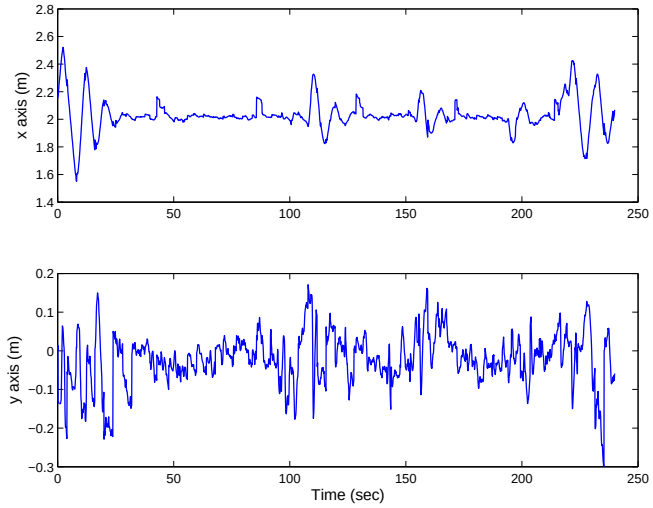

Fig. 5. Time evolution of the estimates for the relative position of the leader with respect to the rear robot.

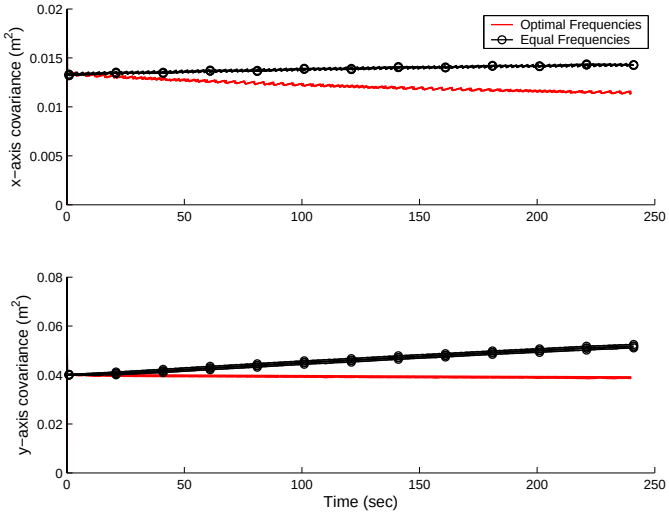

Fig. 6. Comparison of the covariance values that arise when using the optimal measurement frequencies (solid lines) vs. equal measurement frequencies for all exteroceptive measurements (dashed lines with circles). The two plots correspond to the covariance along the x- and y-axis respectively, for all robots.

relative poses of the robots, the covariance of the relative pose measurements was also time-varying, since the number of laser points used for linefitting was not constant for each robot pair. It is significant to observe that despite these differences from the nominal values, the theoretically predicted covariance is very close to the actual one, which verifies the applicability of our approach to practical scenarios.

In order to demonstrate the positioning accuracy improvement that is achieved using the proposed optimization algorithm, we compare the performance of the optimal strategy with that of an "intuitive" strategy, where the available resources are divided equally among all the available measurements (i.e., when we use all measurements at the same rate, $f_j = 3/7$ Hz). In Fig. 6, the time evolution of the covariance in these two scenarios is shown. As evident, there is a clear improvement of performance by using the frequency values produced by the proposed algorithm. Evaluating the *steady-state* covariance attained with the equal-frequency strategy shows that it is approximately 130% and 50% larger along the x and y axes, respectively, compared to the optimal values obtained with our approach. Due to the slow transient response of the covariance, the steady-state value for the case of equal frequencies is not reached in the duration of this experiment. This explains the smaller difference in covariance between the optimal and the "intuitive" approach that appears in Fig. 6.

VII. Simulation Results

This section presents simulation results that demonstrate certain additional interesting properties of the problem of determining the optimal sensing frequencies for groups of robots. We here consider a formation with the same geometry as the one shown in Fig. 3, but we now examine the case where all robots are equipped with a distance and a bearing sensor, that are capable of providing independent measurements, with standard deviations $\sigma_\rho = 0.05$m, and $\sigma_\theta = 1^o$, respectively. Additionally, we assume that all robots have a 360^o field of view, and can potentially record relative measurements of

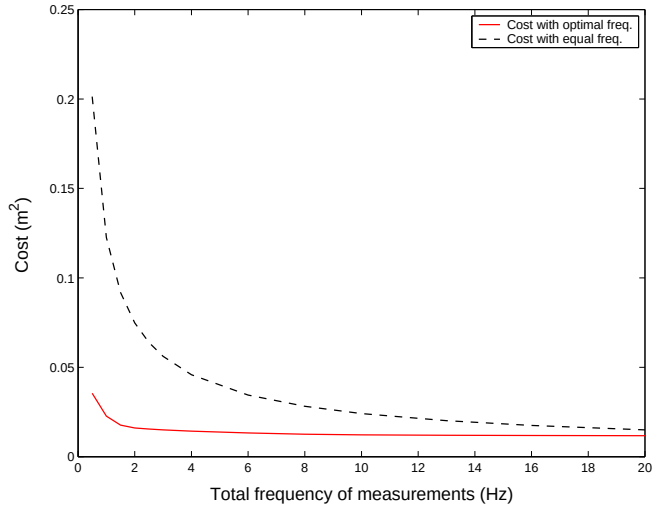

Fig. 7. Cost function vs. Total frequency of measurements.

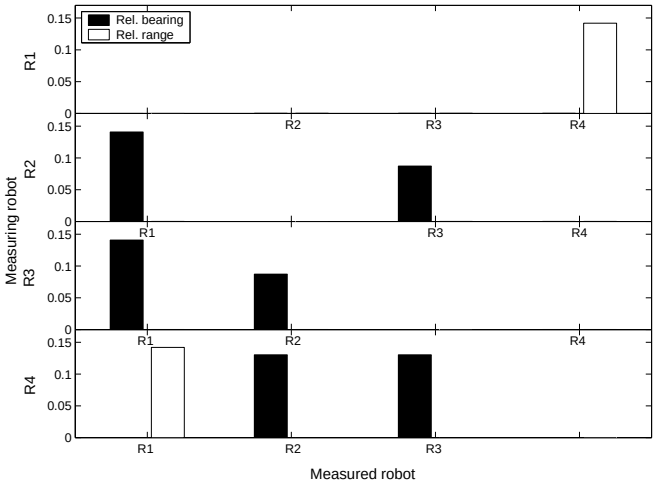

Fig. 8. Optimal values for the relative range and bearing frequencies.

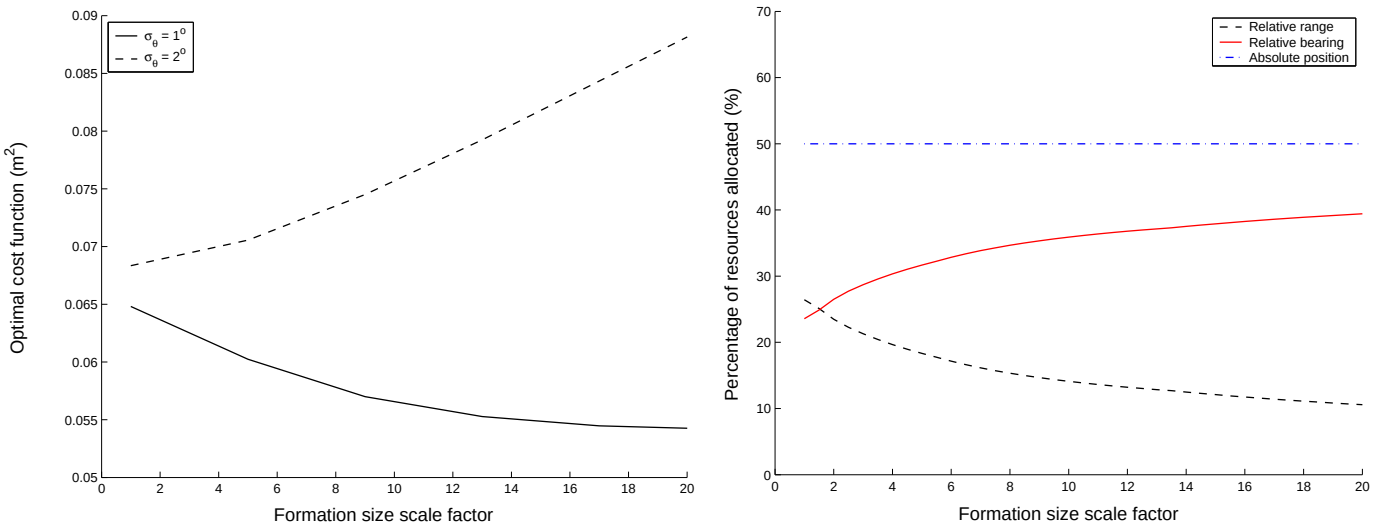

(a) (b)

Fig. 9. (a) The optimal cost as a function of the formation size, for two values of the relative bearing errors' standard deviation. (b) The percentage of resources allocated to each type of measurement, as a function of the formation size, for $\sigma_\theta = 1^\circ$.

all other robots. The leader robot receives absolute position measurements with standard deviations equal to $\sigma_p = 0.3$m along each axis, and absolute orientation measurements with standard deviation $\sigma_\phi = 3^\circ$. The maximum frequency of all measurements is equal to 1Hz, and the threshold on the orientation variance for the robots, is equal to $\epsilon_\phi = 0.0027\text{rad}^2$, corresponding to a standard deviation of 3°.

We first examine the effect of varying the total frequency of measurements processed by the robots. In Fig. 7, the optimal value of the cost function is plotted as a function of the total frequency of measurements (solid line) ($f_{\text{total}} = 0.5 \ldots 20$Hz), and compared to the cost that arises if equal measurement frequencies are employed (dashed line). In this plot, the substantial improvement in localization accuracy attained using our method becomes apparent. For example, for $f_{\text{total}} = 1$Hz, the cost when using equal frequencies is 560% larger than when using the optimal frequencies. Moreover, in this plot we observe a law of diminishing return: there is a sharp improvement in performance by increasing the total number of measurements per time step, when this number is small, but the incremental gain reduces as the frequency of measurements increases further. Since the necessary communication and computational resources increase linearly with the number of measurements performed by the robots, it becomes clear that unless resources are abundant, it is not beneficial for the robots to process a very large number of measurements.

We now constrain the total frequency of measurements to be equal to $f_{\text{total}} = 2$Hz, and run the optimization algorithm. At the optimal solution, the GPS receiver is utilized at its maximum frequency ($f_{GPS} = 1$Hz), and interestingly, *no absolute orientation* measurements need to be recorded. The optimal frequencies for the range and bearing measurements are shown in Fig. 8, in the form of a bar plot, where each row of the plot corresponds to the measurements recorded by one robot. The fact that no absolute orientation measurements are used implies that the correlations between the position and orientation estimates of the robots suffice for guaranteing orientation variance smaller than ϵ_ϕ for all robots. However, it should be made clear that this is *not* a general result. For example, if we double the standard deviation of the absolute position measurements, the results of the optimization under the same conditions show that absolute orientation measurements *are* processed by the robots. Nevertheless, the fact that for certain formations some measurement frequencies may turn out to be equal to zero implies that the corresponding sensors are *not necessary*, and can be omitted, thus resulting in lower cost and easier implementation.

In the last set of experiments, we assume that no absolute orientation sensors are available to the robots, and thus the absolute position measurements of R_1 constitute the only source of absolute state information. We once again select $f_{\text{total}} = 2$Hz, and vary the formation size, by scaling all distances among robots by a factor ranging between 1 and 20. The solid line in Fig. 9(a) presents the optimal cost as a function of the formation size, for $\sigma_\theta = 1^\circ$. It is worth noting that in this case as the formation scale factor increases, the robots' localization accuracy becomes *better*. This is attributed to the fact that in the sensor model for relative measurements, the noise variance is independent of the distance between robots. Therefore, the bearing measurements provide better orientation information for the measuring robot, as the robots get further apart, since the errors in the measured robot's position have less impact. This interpretation is also corroborated by Fig. 9(b) where we plot the proportion of resources (i.e., proportion of the total measurement frequency) assigned to each type of measurement, as the formation size increases. We observe that as robots become more distant, more relative bearing information is utilized. However this is, once again, not a general result: if we increase the standard deviation of the bearing measurements by a mere factor of 2, to $\sigma_\theta = 2^\circ$, then as the formation becomes larger, the robots' localization accuracy degrades (this is shown by the dashed

line in Fig. 9(a)). In this case, the bearing measurements contribute less localization information, and cannot compensate for the loss of information in the range measurements, due to the increased distances among robots.

As a closing remark, we note that the parameters affecting the selection of optimal measurement frequencies include the number of robots, the size and geometric configuration of the formation in space, the robots' velocity, the accuracy of all available sensors, the type and number of available measurements, and the maximum frequency of each sensor. The results presented in this section illustrate the fact that the interactions between these factors are quite intricate, and determining general "rules of thumb" for the optimal sensing strategy appears difficult, if not infeasible. This further establishes the necessity for a design tool that allows, given all the relevant parameters of a particular robot team, to determine measurement strategies that are *provably optimal*. In this work, we have presented a method that yields these optimal results, within the described problem formulation.

VIII. Conclusions

In this paper, we present a new approach to the resource-constrained localization problem for formations of mobile robots. We consider heterogeneous groups of robots equipped with sensors that provide both relative and absolute information. In our formulation the *rates* at which the measurements from individual sensors are utilized are the design variables, and these rates are determined by a trade-off between the localization information each sensor provides, and the cost of processing its measurements. The basis of our approach for determining the optimal sensing strategy is the transition from the discrete-time system model, whose study is analytically intractable, to a *continuous-time* one. The frequency at which each sensor input is processed specifies the accuracy of the corresponding measurement in the continuous-time model. This relation enables us to formulate a *convex optimization problem* for the measurement frequencies, where the constraints on the communication, processing, and power resources of the team are naturally incorporated. Moreover, this problem can be cast as a semidefinite programming (SDP) problem, whose unique global solution can be computed using well-studied and very efficient minimization algorithms.

The results of our work can be employed in practice for determining the sensing frequencies for robot formations of any size and shape comprised of robots with various types of sensors and sensing capabilities. The optimal sensing frequencies can be used not only for obtaining the best localization results, but also for determining the necessity of certain sensors (e.g., sensors with zero frequency can be omitted) which can lead to significant cost savings. Suboptimal solutions, accompanied by a measure of performance loss, are easy to compute based on the properties of the semidefinite optimization problem, and can be employed in scenarios where the time to compute a solution is of critical importance. In our future work, it is our intention to capitalize on this methodology and expand our results to groups of robots that have no access to absolute position data. In this case the problem formulation will be modified so as to express the optimization criterion as a function of the covariance of the pose estimates with respect to one of the robots in the team (relative localization). Moreover, we should point out that the applicability of the proposed method is not limited to the problem of formation localization. The idea of employing a transition from the discrete-time to a continuous-time system model is general, and can be applied to any scheduling problem for which the continuous-time system is linear time invariant.

Appendix I

In this appendix, we prove that the objective value corresponding to the point $Y^\star = (f_1^\star, \ldots, f_M^\star, \mathbf{P}_{ss}^\star)$, with $\mathbf{P}_{ss}^\star$ defined in Eq. (47), is equal to the optimal objective value for problem (46), i.e., that

$$\mathbf{W}_p \mathbf{P}_{ss}^\star \mathbf{W}_p^T \;=\; \mathbf{W}_p \mathcal{P}^\star \mathbf{W}_p^T \tag{49}$$

To simplify the notation, in the following derivations we employ the substitutions $C = \sum_{i=1}^M f_i C_i$ and $C^\star = \sum_{i=1}^M f_i^\star C_i$. In order to prove Eq. (49) we will employ three intermediate results:

Derivation of first result: Pre- and post-multiplying Eq. (45) by $\mathbf{J}^{-1}$ results in the equivalent matrix inequality:

$$-\mathbf{F}_c \mathbf{J}^{-1} - \mathbf{J}^{-1}\mathbf{F}_c^T - \mathbf{Q}_c + \mathbf{J}^{-1} C \mathbf{J}^{-1} \;\succeq\; \mathbf{0}$$

Thus, at the optimal solution, we obtain

$$\mathbf{F}_c \mathbf{J}^{\star-1} + \mathbf{J}^{\star-1}\mathbf{F}_c^T + \mathbf{Q}_c - \mathbf{J}^{\star-1} C^\star \mathbf{J}^{\star-1} = A$$

where $A \preceq \mathbf{0}$. If we denote $\mathbf{Q}_c' = \mathbf{Q}_c - A$, then it is $\mathbf{Q}_c' \succeq \mathbf{Q}_c$, and we see that $\mathbf{J}^{\star-1}$ satisfies an ARE given by

$$\mathbf{F}_c \mathbf{J}^{\star-1} + \mathbf{J}^{\star-1}\mathbf{F}_c^T + \mathbf{Q}_c' - \mathbf{J}^{\star-1} C^\star \mathbf{J}^{\star-1} = \mathbf{0}$$

It can be shown, that the solution of an algebraic Riccati equation is a monotonically increasing function of $\mathbf{Q}_c$ [30]. Therefore, by comparison of the last ARE to the ARE in Eq. (47), we conclude that

$$\mathbf{J}^{\star-1} \succeq \mathbf{P}_{ss}^\star \Rightarrow \mathbf{J}^\star \preceq \mathbf{P}_{ss}^{\star-1} \tag{50}$$

Additionally, from the property $\mathbf{J}^{\star-1} \succeq \mathbf{P}_{ss}^\star$ we derive the first intermediate result:

$$\mathbf{W}_p \mathbf{J}^{\star-1} \mathbf{W}_p^T \succeq \mathbf{W}_p \mathbf{P}_{ss}^\star \mathbf{W}_p^T \tag{51}$$

Derivation of second result: The Karush-Kuhn-Tucker (KKT) optimality conditions [31] for problem (46) include the following "complementary slackness" conditions:

$$\operatorname{trace}(\Lambda_1^\star(\mathbf{J}^{\star-1} - \mathcal{P}^\star)) = 0 \tag{52}$$

$$\operatorname{trace}\left(\Lambda_2^\star \left(\mathbf{J}^\star \mathbf{F}_c + \mathbf{F}_c^T \mathbf{J}^\star - \; C^\star + \mathbf{J}^\star \mathbf{Q}_c \mathbf{J}^\star\right)\right) = 0 \tag{53}$$

$$\lambda_i^\star f_i^\star = 0, \quad i = 1 \ldots M$$

$$\mu_i^\star (f_i^\star - f_{i_{\max}}) = 0, \quad i = 1 \ldots M$$

$$\nu^\star \left(\sum_{i=1}^M f_i^\star - f_{\text{total}} \right) = 0$$

$$\xi_i^\star \left(e_{3i}^T \mathcal{P}^\star e_{3i} - \epsilon_\phi \right) = 0, \quad i = 1 \ldots N$$

as well as the "stationarity" condition:

$$\begin{aligned}&\nabla \operatorname{trace}(\mathbf{W}_p\mathcal{P}\mathbf{W}_p^T) + \nabla \operatorname{trace}\left(\Lambda_1^\star\left(\mathbf{J}^{-1}-\mathcal{P}\right)\right)\\&+\nabla \operatorname{trace}\left(\Lambda_2^\star\left(\mathbf{J}\mathbf{F}_c+\mathbf{F}_c^T\mathbf{J}-C+\mathbf{J}\mathbf{Q}_c\mathbf{J}\right)\right)\\&-\sum_{i=1}^{M}\nabla\lambda_i^\star f_i+\sum_{i=1}^{M}\nabla\mu_i^\star(f_i-f_{i_{\max}})\\&+\nabla\nu^\star\left(\sum_{i=1}^{M}f_i-f_{\text{total}}\right)+\sum_{i=1}^{N}\nabla\xi_i^\star\left(e_{3i}^T\mathcal{P}e_{3i}-\epsilon_\phi\right)=0\end{aligned} \tag{54}$$

where $\Lambda_1, \Lambda_2 \in \mathbf{S}_+^{3N}$, and $\lambda_i,\ \mu_i,\ \nu,\ \xi_i \geq 0$ are the variables of the dual problem, and the superscript * indicates the value of a variable at the optimal solution. In the Eq. (54) differentiation is with respect to the primal variables $\mathcal{P}$, $\mathbf{J}$, f_i, and the derivatives are computed at the optimal solution. Applying the derivative with respect to $\mathcal{P}$, and evaluating at the optimal point, yields:

$$\begin{aligned}&\mathbf{0}=\mathbf{W}_p\mathbf{W}_p^T-\Lambda_1^\star+\sum_{i=1}^{N}\xi_i^\star e_{3i}e_{3i}^T\Rightarrow\\&\Lambda_1^\star=\mathbf{W}_p\mathbf{W}_p^T+\sum_{i=1}^{N}\xi_i^\star e_{3i}e_{3i}^T\ \Rightarrow\ \Lambda_1^\star=\mathbf{W}_p'\mathbf{W}_p'^T\end{aligned} \tag{55}$$

where $\mathbf{W}_p'$ is a diagonal matrix, whose diagonal elements corresponding to the robots' positions are equal to 1, while the elements corresponding to the robots' orientation are equal to $\sqrt{\xi_i^\star}$, $i = 1 \ldots N$.

We now employ the KKT complementary slackness condition with respect to the dual variable Λ_1 (Eq. (52)), to obtain:

$$\begin{aligned}\operatorname{trace}(\Lambda_1^\star(\mathcal{P}^\star-\mathbf{J}^{\star-1}))&=0\Rightarrow\\\operatorname{trace}(\mathbf{W}_p'^T(\mathcal{P}^\star-\mathbf{J}^{\star-1})\mathbf{W}_p')&=0\Rightarrow\\\mathbf{W}_p'^T(\mathcal{P}^\star-\mathbf{J}^{\star-1})\mathbf{W}_p'&=\mathbf{0}\end{aligned} \tag{56}$$

This result follows from the fact that for any symmetric (positive or negative) semidefinite matrix A,

$$\operatorname{trace}(A)=0\Rightarrow A=\mathbf{0}$$

Pre- and post-multiplying Eq. (56) by $\mathbf{W}_p = \mathbf{W}_p^T$, and using the fact that $\mathbf{W}_p\mathbf{W}_p' = \mathbf{W}_p$, we obtain the second intermediate result:

$$\mathbf{W}_p\mathcal{P}^\star\mathbf{W}_p^T=\mathbf{W}_p\mathbf{J}^{\star-1}\mathbf{W}_p^T \tag{57}$$

Derivation of third result: Applying Eq. (54) for the derivative with respect to $\mathbf{J}$, and evaluating at the optimal solution, yields

$$-\mathbf{J}^{\star-1}\Lambda_1^\star\mathbf{J}^{\star-1}+\mathbf{F}_c^T\Lambda_2^\star+\Lambda_2^\star\mathbf{F}_c+\Lambda_2^\star\mathbf{J}^\star\mathbf{Q}_c+\mathbf{Q}_c\mathbf{J}^\star\Lambda_2^\star=\mathbf{0} \tag{58}$$

We now pre-multiply Eq. (47) by $\Lambda_2^\star\mathbf{P}_{ss}^{\star-1}$, post-multiply by $\mathbf{P}_{ss}^{\star-1}$, and apply the trace operator, to obtain the identity

$$\operatorname{trace}\left(\Lambda_2^\star\left(\mathbf{P}_{ss}^{\star-1}\mathbf{F}_c+\mathbf{F}_c^T\mathbf{P}_{ss}^{\star-1}-C^\star+\mathbf{P}_{ss}^{\star-1}\mathbf{Q}_c\mathbf{P}_{ss}^{\star-1}\right)\right)=0$$

Subtracting this equation from the second complementary slackness condition (Eq. (53)), and rearranging terms, we find

$$\begin{aligned}\operatorname{trace}\Big(\left(\mathbf{J}^\star-\mathbf{P}_{ss}^{\star-1}\right)\left(\Lambda_2^\star\mathbf{F}_c+\mathbf{F}_c^T\Lambda_2^\star+\right.\\\left.\Lambda_2^\star\mathbf{J}^\star\mathbf{Q}_c+\mathbf{Q}_c\mathbf{P}_{ss}^{\star-1}\Lambda_2^\star\right)\Big)=0\end{aligned} \tag{59}$$

Using the result of Eq. (58) to simplify this expression, and separating terms, yields

$$\begin{aligned}&\operatorname{trace}\Big(\left(\mathbf{J}^\star-\mathbf{P}_{ss}^{\star-1}\right)\mathbf{J}^{\star-1}\Lambda_1^\star\mathbf{J}^{\star-1}\Big)\\&\qquad=\operatorname{trace}\Big(\left(\mathbf{J}^\star-\mathbf{P}_{ss}^{\star-1}\right)\mathbf{Q}_c(\mathbf{J}^\star-\mathbf{P}_{ss}^{\star-1})\Lambda_2^\star\Big)\end{aligned} \tag{60}$$

At this point, we note that the right-hand side of this equation is a nonnegative quantity, since the matrices $\left(\mathbf{J}^\star-\mathbf{P}_{ss}^{\star-1}\right)\mathbf{Q}_c(\mathbf{J}^\star-\mathbf{P}_{ss}^{\star-1})$ and $\Lambda_2^\star$ are symmetric positive semidefinite. We now show that the left hand side of Eq. (60) is nonpositive. Using the expression of Eq. (55), as well as the property $\mathbf{J}^\star \preceq \mathbf{P}_{ss}^{\star-1}$ (cf. Eq. (50)), we obtain

$$\begin{aligned}\alpha&=\operatorname{trace}\left(\left(\mathbf{J}^\star-\mathbf{P}_{ss}^{\star-1}\right)\mathbf{J}^{\star-1}\Lambda_1^\star\mathbf{J}^{\star-1}\right)\\&=\operatorname{trace}\left(\mathbf{W}_p'^T\mathbf{J}^{\star-1}\left(\mathbf{J}^\star-\mathbf{P}_{ss}^{\star-1}\right)\mathbf{J}^{\star-1}\mathbf{W}_p'\right)\preceq 0\end{aligned}$$

Combining this last result and the fact that the right-hand side of Eq. (60) is a nonnegative quantity, we conclude that both sides must be equal to zero. Consequently,

$$\begin{aligned}\mathbf{W}_p'^T\mathbf{J}^{\star-1}\left(\mathbf{J}^\star-\mathbf{P}_{ss}^{\star-1}\right)\mathbf{J}^{\star-1}\mathbf{W}_p'&=\mathbf{0}\Rightarrow\\\mathbf{W}_p'^T\mathbf{J}^{\star-1}\mathbf{W}_p'-\mathbf{W}_p'^T\mathbf{J}^{\star-1}\mathbf{P}_{ss}^{\star-1}\mathbf{J}^{\star-1}\mathbf{W}_p'&=\mathbf{0}\end{aligned} \tag{61}$$

We now consider the following matrix:

$$\mathbf{E}=\begin{bmatrix}\mathbf{P}_{ss}^\star & -\mathbf{J}^{\star-1}\mathbf{W}_p'\\-\mathbf{W}_p'^T\mathbf{J}^{\star-1} & \mathbf{W}_p'^T\mathbf{J}^{\star-1}\mathbf{W}_p'\end{bmatrix}$$

Applying the lemma of Appendix II, we see that the minimum value of the quadratic product $[u^T \quad v^T]\mathbf{E}[u^T \quad v^T]^T$ over all vectors $[u^T \quad v^T]^T$ is equal to

$$v^T\left(\mathbf{W}_p'^T\mathbf{J}^{\star-1}\mathbf{W}_p'-\mathbf{W}_p'^T\mathbf{J}^{\star-1}\mathbf{P}_{ss}^{\star-1}\mathbf{J}^{\star-1}\mathbf{W}_p'\right)v$$

Using the result of Eq. (61) we conclude that the minimum value of the quadratic product $[u^T \quad v^T]\mathbf{E}[u^T \quad v^T]^T$ equals zero, and thus $\mathbf{E}$ is positive semidefinite. Therefore

$$\begin{aligned}\begin{bmatrix}\mathbf{W}_p & \mathbf{W}_p\end{bmatrix}\mathbf{E}\begin{bmatrix}\mathbf{W}_p & \mathbf{W}_p\end{bmatrix}^T&\succeq\mathbf{0}\Rightarrow\\\mathbf{W}_p\mathbf{P}_{ss}^\star\mathbf{W}_p^T-\mathbf{W}_p\mathbf{J}^{\star-1}\mathbf{W}_p^T&\succeq\mathbf{0}\\\mathbf{W}_p\mathbf{P}_{ss}^\star\mathbf{W}_p^T&\succeq\mathbf{W}_p\mathbf{J}^{\star-1}\mathbf{W}_p^T\end{aligned} \tag{62}$$

where we have used the fact that $\mathbf{W}_p'\mathbf{W}_p = \mathbf{W}_p$. Eq. (62) is the third intermediate result.

Proof of Eq. (49)*:* Substituting from Eq. (57) in Eqs. (51) and (62) we obtain

$$\mathbf{W}_p\mathcal{P}^\star\mathbf{W}_p^T\succeq\mathbf{W}_p\mathbf{P}_{ss}^\star\mathbf{W}_p^T$$

and

$$\mathbf{W}_p\mathbf{P}_{ss}^\star\mathbf{W}_p^T\succeq\mathbf{W}_p\mathcal{P}^\star\mathbf{W}_p^T$$

respectively. The desired result of Eq. (49) follows directly from the last two relations.

APPENDIX II

It can be easily shown that if $A \succ \mathbf{0}$, and D is symmetric, then for any vector y of appropriate dimensions, the minimum of

$$\begin{bmatrix}x\\y\end{bmatrix}^T\begin{bmatrix}A & B\\B^T & D\end{bmatrix}\begin{bmatrix}x\\y\end{bmatrix}$$

with respect to x is equal to $y^T\left(D-B^TA^{-1}B\right)y$ and is attained for $x=-A^{-1}By$.

REFERENCES

[1] Z. Wang, Y. Hirata, and K. Kosuge, "Control a rigid caging formation for cooperative object transportation by multiple mobile robots," in *Proc. of the IEEE International Conference on Robotics and Automation*, New Orleans, LA, 2004, pp. 1580–1585.

[2] T. Balch and R. C. Arkin, "Behavior-based formation control for multirobot teams," *IEEE Transactions on Robotics and Automation*, vol. 14, no. 6, pp. 926–939, 1998.

[3] A. Broggi, M. Bertozzi, A. Fascioli, C. G. L. Bianco, and A. Piazzi, "Visual perception of obstacles and vehicles for platooning," *IEEE Transactions on Intelligent Transportation Systems*, vol. 1, no. 3, pp. 164–176, 2000.

[4] S. Venkataramanan and A. Dogan, "Nonlinear control for reconfiguration of UAV formation," in *Proc. of the AIAA Guidance, Navigation, and Control Conference*, Austin, TX, 2003.

[5] J. Adams, A. Robertson, K. Zimmerman, and J. How, "Technologies for spacecraft formation flying," in *Proc. ION-GPS 96*, 1996, pp. 1321–1330.

[6] S. I. Roumeliotis and G. A. Bekey, "Distributed multirobot localization," *IEEE Transactions on Robotics and Automation*, vol. 18, no. 5, pp. 781–795, 2002.

[7] A. Das, J. Spletzer, V. Kumar, and C. Taylor, "Ad hoc networks for localization and control," in *Proc. of the 41st IEEE Conference on Decision and Control*, Las Vegas, NV, 2002, pp. 2978– 2983.

[8] D. Fox, W. Burgard, H. Kruppa, and S. Thrun, "A probabilistic approach to collaborative multi-robot localization," *Autonomous Robots*, vol. 8, no. 3, pp. 325–344, 2000, special Issue on Heterogeneous Multirobot Systems.

[9] J. Spletzer, A. Das, R. Fierro, C. Taylor, V. Kumar, and J. Ostrowski, "Cooperative localization and control for multi-robot manipulation," in *Proc. of IEEE/RSJ International Conference on Intelligent Robots and Systems*, Wailea, HI, 2001, pp. 631 – 636.

[10] A. Das, R. Fierro, V. Kumar, J. Ostrowski, J. Spletzer, and C. Taylor, "A vision-based formation control framework," *IEEE Transactions on Robotics and Automation*, vol. 18, no. 5, pp. 813 – 825, 2002.

[11] F. Zhang, B. Grocholsky, and V. Kumar, "Formations for localization of robot networks," in *Proc. of the IEEE International Conference on Robotics and Automation*, New Orleans, LA, 2004, pp. 3369–3374.

[12] Y. S. Hidaka, A. I. Mourikis, and S. I. Roumeliotis, "Optimal formations for cooperative localization of mobile robots," in *Proc. of the IEEE International Conference on Robotics and Automation*, Barcelona, Spain, 2005, pp. 4137–4142.

[13] R. Kurazume and S. Hirose, "Study on cooperative positioning system: optimum moving strategies for CPS-III." in *Proc. of the IEEE International Conference in Robotics and Automation*, Leuven, Belgium, 1998, pp. 2896–2903.

[14] C. Kwok, D. Fox, and M. Meila, "Real time particle filters," in *Advances in Neural Information Processing Systems 15 (NIPS)*, 2003, pp. 1057–1064.

[15] L. Meier, J. Peschon, and R. M. Dressler, "Optimal control of measurement subsystems," *IEEE Transactions on Automatic Control*, vol. 12, no. 5, pp. 528–536, 1967.

[16] T. H. Chung, V. Gupta, B. Hassibi, J. W. Burdick, and R. M. Murray, "Scheduling for Distributed Sensor Networks with Single Sensor Measurement Per Time Step," in *Proc. of the IEEE International Conference on Robotics and Automation*, New Orleans, LA, 2004, pp. 187–192.

[17] D. Avintzour and S. Rogers, "Optimal measurement scheduling for prediction and estimation," *IEEE Transactions on Acoustics, Speech, and Signal Processing*, vol. 38, no. 10, pp. 2017–2023, 1990.

[18] H. Lee, K. Teo, and A. E. Lim, "Sensor scheduling in continuous time," *Automatica*, no. 37, pp. 2017–2023, 2001.

[19] E. Skafidas and A. Nerode, "Optimal measurement scheduling in linear quadratic gaussian control problems," in *Proc. of the IEEE International Conference on Control Applications*, Trieste, Italy, 1998, pp. 1225 – 1229.

[20] A. V. Savkin, R. J. Evans, and E. Skafidas, "The problem of optimal sensor scheduling," *Systems and Control Letters*, vol. 43, pp. 149–157, 2001.

[21] J. S. Baras and A. Bensoussan, "Optimal sensor scheduling in nonlinear filtering of diffusion processes," *SIAM Journal of Control and Optimization*, vol. 27, no. 4, pp. 786–813, 1989.

[22] V. Gupta, T. Chung, B. Hassibi, and R. M. Murray, "Sensor scheduling algorithms requiring limited computation," in *Proc. of the IEEE International Conference on Acoustics, Speech and Signal Processing*, Montreal, Canada, 2004, pp. 825–828.

[23] V. Gupta, T. H. Chung, B. Hassibi, and R. M. Murray, "On a stochastic sensor selection algorithm with applications in sensor scheduling and sensor coverage," *Automatica*, vol. 42, 2006.

[24] A. I. Mourikis and S. I. Roumeliotis, "Analysis of Positioning Uncertainty in Reconfigurable Networks of Heterogeneous Mobile Robots," in *Proc. of the 2004 IEEE International Conference on Robotics and Automation*, New Orleans, LA, 2004, pp. 572–579.

[25] ——, "Performance analysis of multirobot cooperative localization," *IEEE Transactions on Robotics*, 2006, to appear.

[26] G. Anousaki and K. J. Kyriakopoulos, "A dead-reckoning scheme for skid-steered vehicles in outdoor environments," in *Proc. of the IEEE International Conference on Robotics and Automation*, New Orleans, LA, 2004, pp. 580–585.

[27] S. Thrun, W. Burgard, and D. Fox, *Probabilistic Robotics*. MIT Press, 2005.

[28] P. S. Maybeck, *Stochastic Models, Estimation, and Control*. Academic Press, 1979, vol. 141-1.

[29] W. L. Brogan, *Modern Control Theory*. Prentice Hall, 1991.

[30] G. Freiling and V. Ionescu, "Monotonicity and convexity properties of matrix Riccati equations," *IMA Journal of Mathematical Control and Information*, no. 18, pp. 61–72, 2001.

[31] S. Boyd and L. Vandenberghe, *Convex Optimization*. Cambridge University Press, 2004.

[32] A. I. Mourikis and S. I. Roumeliotis, "Optimal sensing strategies for mobile robot formations: Resource-constrained localization," in *Proc. of Robotics: Science and Systems*, Cambridge, MA, 2005, pp. 281–288.

[33] H. G. Tanner, G. J. Pappas, and V. Kumar, "Leader-to-formation stability," *IEEE Transactions on Robotics and Automation*, vol. 20, no. 3, pp. 433–455, 2004.

Anastasios I. Mourikis Anastasios Mourikis received the Diploma of Electrical and Computer Engineering with honors from the University of Patras, Greece in 2003. He is currently a PhD candidate at the Department of Computer Science and Engineering (CSE) at the University of Minnesota. His research interests lie in the areas of Localization in Single- and Multi-robot systems, Vision-aided Inertial Navigation, Simultaneous Localization and Mapping, and Structure from Motion. He is the recipient of the 2005 Excellence in Research Award Fellowship from the CSE Department of the University of Minnesota.

Stergios I. Roumeliotis Stergios Roumeliotis received his Diploma in Electrical Engineering from the National Technical University of Athens, Greece, in 1995, and the M.S. and Ph.D. degrees in Electrical Engineering from the University of Southern California, CA in 1997 and 2000 respectively. From 2000 to 2002 he was a postdoctoral fellow at the California Institute of Technology, CA. Since 2002 he has been an Assistant Professor at the Department of Computer Science and Engineering at the University of Minnesota. He is the recipient of the McKnight Land-Grant Professorship award, and the NASA Tech Briefs award. His research interests include inertial navigation of aerial and ground autonomous vehicles, fault detection and identification, and sensor networks. Recently his research has focused on distributed estimation under communication and processing constraints and active sensing for reconfigurable networks of mobile sensors.